CHEMICAL ENGINEERING TRANSACTIONS
VOL. 94, 2022
A publication of AIDIC
The Italian Association of Chemical Engineering
Online at www.cetjournal.it
Guest Editors: Petar S. Varbanov, Yee Van Fan, Jiří J. Klemeš, Sandro Nižetić

ISBN 978-88-95608-93-8; **ISSN** 2283-9216
DOI: 10.3303/CET2294135

A Prediction Model for Temperature Variation and Distribution Using Soft Sensing Method

Feng Xu[a], Yuki Sato[a], Yuka Sakai[a], Shunsuke Sabu[b], Hiroaki Kanayama[b], Daisuke Satou[b], Yasuki Kansha[a,b]*

[a]Organization for Programs on Environmental Sciences, Graduate School of Arts and Sciences, The University of Tokyo, 3-8-1 Komaba, Meguro-ku, Tokyo 153-8902, Japan
[b]Technology and Innovation Center, Daikin Industries, LTD., 1-1 Nishi-Hitotsuya, Settsu, Osaka 566-8585, Japan
kansha@global.c.u-tokyo.ac.jp

Excessively high or low local indoor temperature causes discomfort to the users and wastes energy. Thus, it is significant to use an accurate and fast soft sensor to measure and control the local indoor temperature. In this research, the temperature variation and distribution were experimentally investigated, and an inferential model was developed as a soft sensor to predict the local temperature. To simulate the indoor temperature environment under refrigeration mode of air conditioner, 10 °C cold water was continuously fed to an acrylic box filled with water at two initial temperatures of 25/35 °C. Transient temperatures of different locations were simultaneously measured and the water flow pattern was observed by the particle image velocimetry method. The correlation coefficients between transient temperatures at different locations were examined for the variable selection. A multiple regression model was developed using the least squares method and validated by the measured transient temperatures. The experimental data agreed well with the prediction model. Therefore, this method can contribute to the air conditioning system design.

1. Introduction

The global warming effect is one of serious environmental problems with the rapid development of society and economy (Kweku et al., 2017). Reducing the emissions of greenhouse gas such as CO_2 is significant and contributes to sustainable development. The energy consumption for buildings mainly attributed to the heating, ventilation, and air conditioning (HVAC) system accounts for about 40% of the global energy consumption (Song et al., 2020). The air conditioning system is controlled by the feedback from physical sensors installed inside the air conditioner (Cheng and Lee, 2014). However, the indoor temperature distribution is not uniform when the air conditioner is under operation (Yang et al., 2022). Excessively high or low local indoor temperature causes discomfort to the users and low efficiency of energy utilization. Thus, prediction and control of the local indoor temperature is significant to obtain acceptable human comfort and an effective energy management. Soft sensor is an inferential model that uses easily measurable variables to predict unmeasurable variables (Souza et al., 2016). This technique has been widely applied for process monitoring and control (Lin et al., 2007). The modelling methods of the soft sensor can be classified into three types: model-based (based on process mechanism), data-driven (based on empirical correlations without any process mechanism), and gray-box (combination of empirical and physical models) (Li et al., 2011). Ploennigs et al. (2011) built a model-based soft sensor to predict the heating energy of rooms by reading simple temperature sensors. A control strategy and computational fluid dynamics (CFD) analysis were combined by Guzmán et al. (2019) to monitor the temperature in greenhouses. Cosoli et al. (2020) developed a data-driven soft sensor for temperature measurement in a brew group of coffee machine. An autoregressive exogenous model was trained by data generated by a numerical model. Ríos-Moreno et al. (2007) used two linear autoregressive models to predict air temperature in classrooms using wind speed, global solar radiation flux, outside air temperature and relative humidity as the input variables. The soft sensor can be considered as an available method for local indoor temperature measurement due to feasibility and economy.

Paper Received: 15 April 2022; Revised: 09 May 2022; Accepted: 03 June 2022
Please cite this article as: Xu F., Sato Y., Sakai Y., Sabu S., Kanayama H., Satou D., Kansha Y., 2022, A Prediction Model for Temperature Variation and Distribution Using Soft Sensing Method, Chemical Engineering Transactions, 94, 811-816 DOI:10.3303/CET2294135

This research aims to develop an inferential model that can calculate the transient local temperature at targeted locations using easily measurable temperature as the input variable. A water experiment was carried out to investigate the temperature variation and distribution in an enclosed space. The water flow pattern was observed by the particle image velocimetry (PIV) method. The correlation coefficients between transient temperatures at different locations were calculated. A multiple regression model based on the knowledge of process mechanism was developed and validated by the experimental data.

2. Methodology

2.1 Experimental apparatus and methods

To simulate the indoor temperature environment under refrigeration mode of air conditioner, an empty acrylic box is assumed as a room and a feed nozzle is assumed as outlet of air conditioner. Figure 1 shows the schematic diagram of the experimental apparatus. Initially, the acrylic box was filled by water with designated temperature to simulate initial indoor temperature environment before air conditioner running. Two initial temperatures of 25 °C and 35 °C were used for experiment. Water in a water container was cooled and circulated by using a water circulator. The flow rate was adjusted by two needle valves to 770 mL/min. After the water in the water container reached about 10 °C, the cold water was fed to the acrylic box by the feed nozzle. Excess water was sucked by an aspirator through a drain nozzle. Temperature data of thermocouples in the acrylic box were simultaneously collected by a data logger with the sampling time of 100 ms. The detail of the acrylic box is shown in Figure 2. The periphery and bottom of the acrylic box were covered with thermal insulation material. Moreover, a thermal insulation board was installed in top inside the acrylic box as the ceiling. 39 (horizontal 13 × vertical 3) thermocouples were installed in the acrylic box with symmetrical layout. The distance between the top, middle and bottom layers was the same. One thermocouple was inserted into the feed nozzle to measure the feed water temperature.

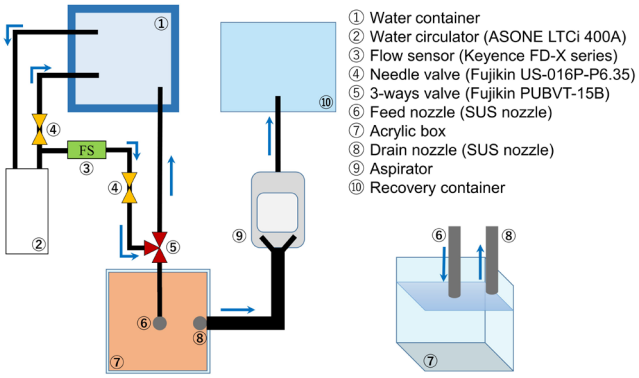

Figure 1: Schematic diagram of the experimental apparatus

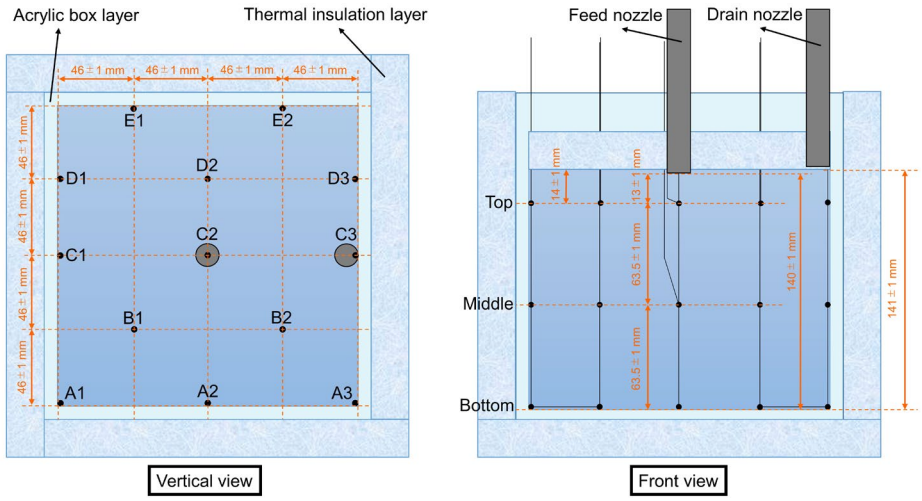

Figure 2: Detail of the acrylic box

The PIV method was used to observe the water flow pattern. A laser source with an intensity of 2.0 A was installed adjacent to the surface of A1, C1, and D1 and vertically illuminated the surface of C1, C2, and C3. A camera with a frame rate of 120 fps was installed in front of the acrylic box to video the water flow pattern of the illuminated surface. Fluorescent red polyethylene (PE) microsphere (diameter: 75-90 μm; density: 0.995 g/cm^3) was used as tracer particle. The PIV experiment was conducted under the same conditions as the temperature experiments mentioned above.

2.2 Inferential model

Considering computation cost, model simplicity, and strong correlation between variables in the process, a multiple linear regression model is used for local temperature prediction, as shown as follows;

$$y = a + bx_1 + cx_2 + dx_3 + \cdots \quad (1)$$

where *y* is the predicted variable and *x* is the measured variable. It is impossible to install a physical sensor in the occupant space of a room corresponding to the interior space of the acrylic box such as the locations of B1 and B2. These local temperatures are the targeted variables. It is not difficult to install a physical sensor to measure the temperature on the room wall. Therefore, the wall temperature of the acrylic box is considered as the measurable variable such as the temperatures of C1, D1, E1, etc. A correlation analysis is conducted to select a suitable measured variable. The correlation coefficient between two temperatures at different locations is calculated as;

$$r_{XY} = \frac{\frac{1}{N}\sum_{i=1}^{N}(X_i - \bar{X})\,(Y_i - \bar{Y})}{\sqrt{\frac{1}{N}\sum_{i=1}^{N}(X_i - \bar{X})^2}\sqrt{\frac{1}{N}\sum_{i=1}^{N}(Y_i - \bar{Y})^2}} \quad (2)$$

Then, transient local temperature can be calculated based on heat transfer process mechanism using the selected measured temperature as the input variable, as shown as follows;

$$T_{predicted} = a + bT_{measured} + c(T_{measured} - T_s) + d\frac{dT_{measured}}{dt} \quad (3)$$

where $T_{measured}$ - T_s represents convective heat transfer term between the measured temperature and the feed temperature, $dT_{measured}/dt$ represents heat conduction term, *a* represents influence or error caused by other parameters such as flow rate and radiation. The measured temperature varied with the elapsed time is fitted by a polynomial equation to obtain the $dT_{measured}/dt$. A gray-box soft sensor for local temperature prediction is developed by arranging the Eq(3), as given by;

$$T_{predicted} = \alpha + \beta T_{measured} + \gamma T_s + \delta\frac{dT_{measured}}{dt} \quad (4)$$

The coefficients α, β, γ, and δ are calculated by the least squares method using the measured data. Due to the symmetrical layout of thermocouples installation and the center layout of the feed nozzle, the temperature data at the locations with the same distance from the feed nozzle and the same distance from the wall of the acrylic box were used for model validation.

3. Results and Discussion

3.1 Experimental results

Figure 3 shows the representative transient temperature of C1T (top), C1M (middle), and C1B (bottom) on the wall of the acrylic box at different initial temperatures of 25 °C and 35 °C. The temperatures of top, middle, and bottom layers decrease from the initial temperature and approach to the feed temperature of 10 °C with the elapsed time. The decrease rates of temperature are different between the layers, but the temperatures of different layers approach to be the same after about 10 min. The temperature of the bottom layer decreases faster than the middle layer and the top layer. The temperature of the middle layer has a little delay before the temperature decrease. An obvious delay is found in the top layer. The delay time of the top layer is different from the initial temperatures. For the initial temperature of 25 °C, the delay time is about 85 s. For the initial temperature of 35 °C, the delay time is about 110 s. Larger temperature difference between the initial temperature and the feed temperature results in a longer delay time for the top layer.

The transient temperatures of other places have a similar trend with C1 except for C2, A1, and A3. The temperatures of C2 are more sensitive and decrease fast without delay because the C2 is located directly below the feed nozzle. For A1 and A3, the temperature of the bottom layer is higher than that of the middle layer because A1B and A3B are located at the corner of the acrylic box.

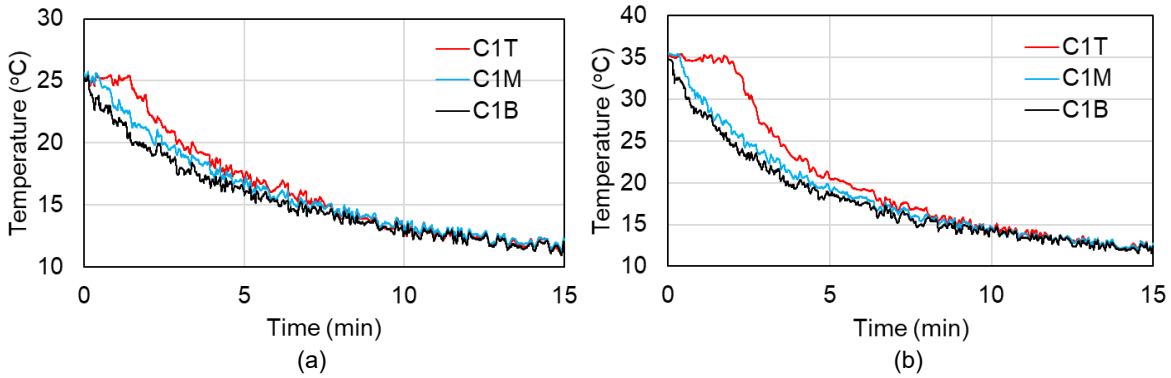

Figure 3: Transient temperature of C1T, C1M, and C1B under different initial temperatures of (a) 25 °C and (b) 35 °C

The flow patterns for the initial temperature of 35 °C at the elapsed time of 1.5 min and 7 min are shown in Figure 4. The red line is the trail of the tracer particle, the green line is the frame of the acrylic box and the top is the ceiling with the feed nozzle inside. The water outflowing from the feed nozzle initially reaches the bottom of the acrylic box due to the forced convection. Then, the cold water flows to the surrounding along the bottom layer. At the elapsed time of 1.5 min, the tracer particles cannot reach the top layer. However, the acrylic box has been filled with tracer particles at the elapsed time of 7 min. This phenomenon is corresponding to the time delay of temperature decrease for the top layer. Due to the density difference between cold and hot water, it takes time for the cold water on the bottom layer to diffuse to the top layer under the natural convection. In addition, the position in the upper right corner of Figure 4b is just below the drain nozzle, which is affected by the water suction.

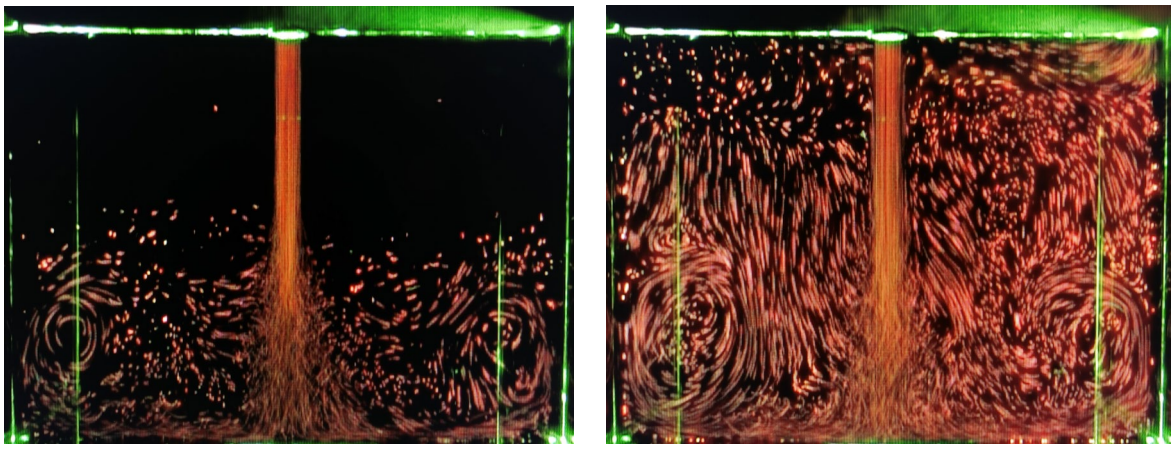

Figure 4: Flow patterns at the elapsed time of (a) 1.5 min and (b) 7 min

3.2 Prediction and validation

Under the initial temperature of 25 °C, the correlation coefficients between C1M and B1T, C1M and B1M, C1M and B1B are 0.978, 0.989, and 0.984, respectively. Under the initial temperature of 35 °C, the correlation coefficients between C1M and B1T, C1M and B1M, C1M and B1B are 0.973, 0.994, and 0.991, respectively. The C1M is selected as the input data due to high positive correlation with B1T, B1M, and B1B. Figure 5a shows the transient temperature prediction for B1M under the initial temperature of 25 °C. The experimental data of B1M and C1M are used as training data to calculate the coefficients of Eq(4). By using the least squares method, the C1M-B1M model is obtained by using the transient temperature of B1M as $T_{predicted}$, the transient temperature of C1M as $T_{measured}$, the transient feed temperature as T_s, as given by;

$$T_{B1M} = 9.592 + 0.260T_{C1M} - 0.146T_s - 201.765\frac{dT_{C1M}}{dt} \quad (5)$$

The predicted data of B1M from Eq(5) agree well with the experimental data with the coefficient of determination (R^2) of 0.988. The temperature difference between experimental data and predicted data (ΔT) can be controlled within ±1 °C for the whole process of 900 s as shown in Figure 5b. The location of A2M is similar to the C1M and the location of B2M is similar to the B1M. For the validation of the C1M-B1M case, the transient temperature of B2M is predicted by the C1M-B1M model using the experimental data of A2M as shown in Figure 6a. The ΔT within ±1 °C means a good agreement between predicted data and experimental data of B2M. The coefficients α, β, γ, δ and R^2 for the case study are shown in Table 1. The R^2 of all cases is high. The ΔT of the middle layer and the bottom layer under two initial temperatures can be controlled within ±1 °C for the whole process of 900 s. The ΔT of B1T under the initial temperature of 25 °C is within ±2 °C before the elapsed time of 124 s and within ±0.5 °C after 215 s. For the case of B1T under the initial temperature of 35 °C, the deviation becomes larger at the initial phase. It is understood that the time delay of temperature decrease for the top layer affects the model accuracy of initial phase. In overall, this soft sensor for local temperature prediction is effective and convenient.

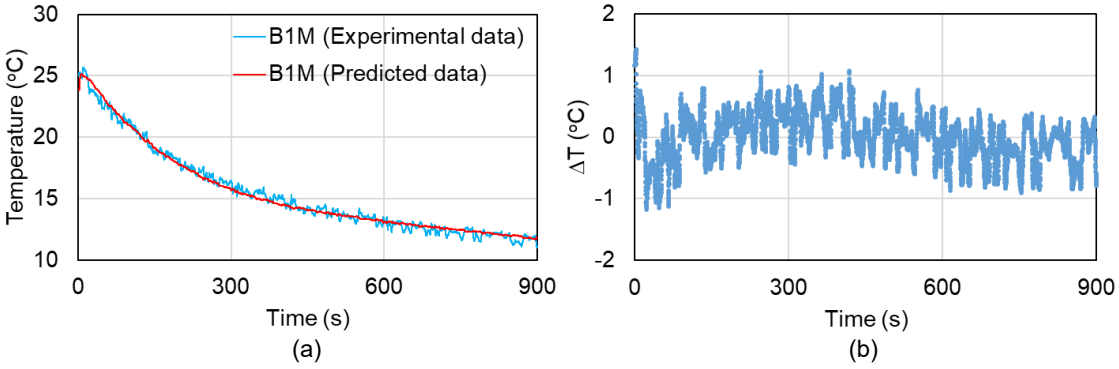

Figure 5: (a) Temperature prediction of B1M (b) Temperature difference between experimental and predicted data of B1M

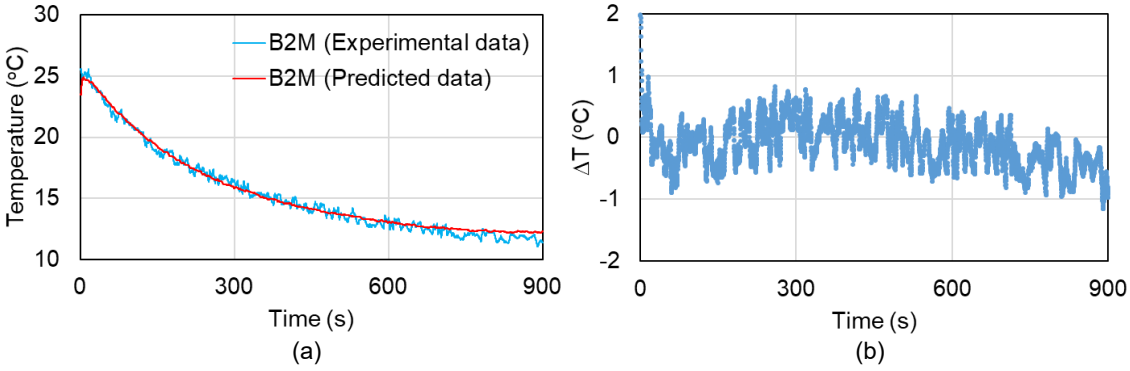

Figure 6: (a) Validation of the inferential model (b) Temperature difference between experimental and predicted data of B2M

Table 1: Coefficients and R^2 of case study

Initial temperature	Predicted location	α	β	γ	δ	R^2
25 °C	B1T	13.775	0.163	-0.532	-299.323	0.978
	B1M	9.592	0.260	-0.146	-201.765	0.988
	B1B	8.795	0.233	-0.048	-182.314	0.979
35 °C	B1T	4.234	1.115	-0.690	-50.582	0.957
	B1M	5.955	0.570	-0.117	-94.423	0.993
	B1B	5.132	0.542	-0.015	-78.872	0.987

4. Conclusions

An experimental and theoretical investigation was carried out to develop a soft sensor for local temperature prediction. A water experiment in an enclosed space was conducted to simulate the indoor temperature

environment under the refrigeration mode of the air conditioner. 10 °C cold water was continuously fed to an acrylic box with two initial temperatures of 25/35 °C. Transient temperatures of 39 points located at different places with three top, middle, and bottom layers in the cubic space were simultaneously measured after the cold water feed started. The temperature of the bottom layer decreased fastest with time except for the corner of the acrylic box and the position just below the feed nozzle. A time delay of temperature decrease was found in the top layer. Under the same conditions, the PIV experiment was conducted to observe the water flow pattern. The correlation coefficients between the measurable variable and targeted variable were positively high. A multiple regression model was developed by considering the heat transfer process mechanism and trained by the measured data using the least squares method. The transient temperatures of B1T, B1M and B1B were predicted by the inferential model with acceptable accuracy. The inferential model was validated by the measured data at similar positions. Therefore, it is considered that this gray-box soft sensor method can be used to predict local indoor temperature. This multiple linear regression model is easy to be integrated into the temperature control unit of the HVAC system. With the feedback of the soft sensor, a better human comfort and a higher energy efficiency can be obtained by a deeper control of temperature management.

Nomenclature

r_{XY} – correlation coefficient
R^2 – coefficient of determination
T_{B1M} – temperature of B1M, °C
T_{C1M} – temperature of C1M, °C
$T_{measured}$ – measured temperature, °C
$T_{predicted}$ – predicted temperature, °C
T_s – feed temperature, °C
ΔT – temperature difference between experimental data and predicted data, °C
x – measured variable
y – predicted variable
α, β, γ, δ – coefficients of the inferential model

Acknowledgments

This research is financially supported by New Energy and Industrial Technology Development Organization, NEDO, Japan.

References

Cheng C., Lee D., 2014, Smart Sensors Enable Smart Air Conditioning Control, Sensors, 14, 11179–11203.
Cosoli G., Chiariotti P., Martarelli M., Foglia S., Parrini M., Tomasini E.P., 2020, Development of a Soft Sensor for Indirect Temperature Measurement in a Coffee Machine, IEEE Transactions on Instrumentation and Measurement, 69(5), 2164–2171.
Guzmán C.H., Carrera J.L., Durán H.A., Berumen J., Ortiz A.A., Guirette O.A., Arroyo A., Brizuela J.A., Gómez F., Blanco A., Azcaray H.R., Hernández M., 2019, Implementation of Virtual Sensors for Monitoring Temperature in Greenhouses Using CFD and Control, Sensors, 19(1), 60.
Kweku D.W., Bismark O., Maxwell A., Desmond K.A., Danso K.B., Oti-Mensah E.A., Quachie A.T., Adormaa B.B., 2017, Greenhouse Effect: Greenhouse Gases and Their Impact on Global Warming, Journal of Scientific Research & Reports, 17(6), 1–9.
Lin B., Recke B., Knudsen J.K.H., Jørgensen S.B., 2007, A Systematic Approach for Soft Sensor Development, Computers and Chemical Engineering, 31, 419–425.
Li H., Yu D., Braun J.E., 2011, A Review of Virtual Sensing Technology and Application in Building Systems, HVAC&R Research, 17(5), 619–645.
Ploennigs J., Ahmed A., Hensel B., Stack P., Menzel K., 2011, Virtual Sensors for Estimation of Energy Consumption and Thermal Comfort in Buildings with Underfloor Heating, Advanced Engineering Informatics, 25, 688–698.
Ríos-Moreno G.J., Trejo-Perea M., Castañeda-Miranda R., Hernández-Guzmán V.M., Herrera-Ruiz G., 2007, Modelling Temperature in Intelligent Buildings by Means of Autoregressive Models, Automation in Construction, 16, 713–722.
Souza F.A.A., Araújo R., Mendes J., 2016, Review of Soft Sensor Methods for Regression Applications, Chemometrics and Intelligent Laboratory Systems, 152, 69–79.
Song K., Jang Y., Park M., Lee H., Ahn J., 2020, Energy Efficiency of End-User Groups for Personalized HVAC Control in Multi-Zone Buildings, Energy, 206, 118116.
Yang Z., Dong X., Xiao H., Sun H., Wang B., Shi W., Li X., 2022, Investigation of Thermal Comfort of Room Air Conditioner During Heating Season, Building and Environment, 207, 108544.